

Structural distortions in the spin-gap regime of the quantum antiferromagnet $\text{SrCu}_2(\text{BO}_3)_2$

C. Vecchini^{a,b,*}, O. Adamopoulos^{a,c}, L.C. Chapon^b, A. Lappas^{a,**}, H. Kageyama^d, Y. Ueda^e, A. Zorko^f

^a Institute of Electronic Structure and Laser, Foundation for Research and Technology–Hellas, Vassilika Voutou, 711 10 Heraklion, Crete, Greece

^b ISIS Facility, Rutherford Appleton Laboratory, Chilton, Didcot, Oxfordshire, OX11 0QX, United Kingdom

^c Department of Chemistry, University of Crete, Voutes, 710 03 Heraklion, Greece

^d Department of Chemistry, Graduate School of Science, Kyoto University, Kyoto 606-8502, Japan

^e Institute of Solid State Physics, University of Tokyo, 5-1-5 Kashiwanoha, Kashiwa, Chiba 277-8581, Japan

^f Institute Jožef Stefan, Jamova 39, 1000 Ljubljana, Slovenia

ARTICLE INFO

Article history:

Received 16 April 2009

Received in revised form

31 August 2009

Accepted 14 September 2009

Available online 19 September 2009

Keywords:

Neutron diffraction

Frustrated system

Antiferromagnet

Two-dimensional system

Dimer

$\text{SrCu}_2(\text{BO}_3)_2$

Spin-gap

Shastry–Sutherland

Strongly correlated systems

ABSTRACT

We report the first crystallographic study within the low-temperature (< 40 K) spin-gap region of the two-dimensional frustrated antiferromagnet $\text{SrCu}_2(\text{BO}_3)_2$. The crystal system does not deviate from the tetragonal $I-42m$ space group symmetry. However, our high-resolution neutron powder diffraction measurements uncover subtle structural modifications below 34 K, concomitant to the formation of the dimer singlet ground state. Intimate spin–lattice coupling leads to negative thermal expansion of the tetragonal structure, which reflects into particular local lattice adjustments. The extracted structural parameters suggest the reduction of the buckling found in the copper–borate planes and the strengthening of the leading, in-plane intra-dimer superexchange interaction. The observed contraction along the c -axis, associated with the inter-dimer exchange in adjacent layers, indicates the involvement of weaker three-dimensional interactions in the magnetic properties. The rules posed by the crystal symmetry do not preclude Dzyaloshinsky–Moriya interactions, which therefore remain as an important source of spin anisotropy necessary to rationalise the ground state behaviour.

© 2009 Elsevier Inc. All rights reserved.

1. Introduction

Low-dimensional systems with a quantum-disordered singlet ground state have attracted much attention in the past years, both from the experimental as well as the theoretical point of view. The Haldane ($S=1$, Y_2BaNiO_5) [1], spin-Peierls ($S = \frac{1}{2}$, CuGeO_3) [2], ladder ($S = \frac{1}{2}$, SrCu_2O_3) [3] and plaquette ($S = \frac{1}{2}$, CaV_4O_9) [4] systems are members of the broader family, with a spin excitation gap from the nonmagnetic singlet ground state to the first excited triplet state. Quantum spin fluctuations and/or magnetic anisotropy often play a decisive role in the determination of the nature of the ground state properties. A rich variety of phenomena have been observed and predicted in this type of materials; therefore, the discovery of other examples of chemical compounds is worthy as it can promote the understanding of fundamental processes governing the spin-dynamics in the quantum critical regime.

More than twenty years ago, Shastry and Sutherland proposed an interesting theoretical model [5]; they calculated the ground state of an anisotropic quantum spin Heisenberg Hamiltonian with next-neighbor interactions in two dimensions. $\text{SrCu}_2(\text{BO}_3)_2$ is a Heisenberg system which displays a unique exchange topology. This compound is indeed one of the first experimental realizations of the two-dimensional (2D) Shastry–Sutherland lattice [6,7], in which a rectangular network of spin-1/2 Cu^{2+} dimers is arranged within a square-based structure with diagonal bonds, allowing for nearest- (J_1 , intra-dimer exchange pathway) and next-nearest- (J_2 , inter-dimer exchange pathway) neighbor dimer interactions (Fig. 1). $\text{SrCu}_2(\text{BO}_3)_2$ presents a dimerized nonmagnetic ground state [8,9], with an energy gap of $\Delta = 34(1)$ K [7,10] between the singlet and the triplet states.

As the strong interplay between the crystal structure and the magnetic properties is a well-known aspect of low-dimensional systems, in the recent years many theoretical works were motivated from the phase diagram of the general Shastry–Sutherland lattice type [11]. For the original 2D model, the exact dimer ground state is realized for small $x = |J_2|/|J_1|$. Although there are still open questions, there is reasonable consent that when the exchange interactions are tuned to a critical value x_c , of about 0.7,

* Corresponding author. Fax: +44 1235 44720.

** Also corresponding author. Fax: +30 2810 391305.

E-mail addresses: carlo.vecchini@stfc.ac.uk (C. Vecchini), lappas@iesl.forth.gr (A. Lappas).

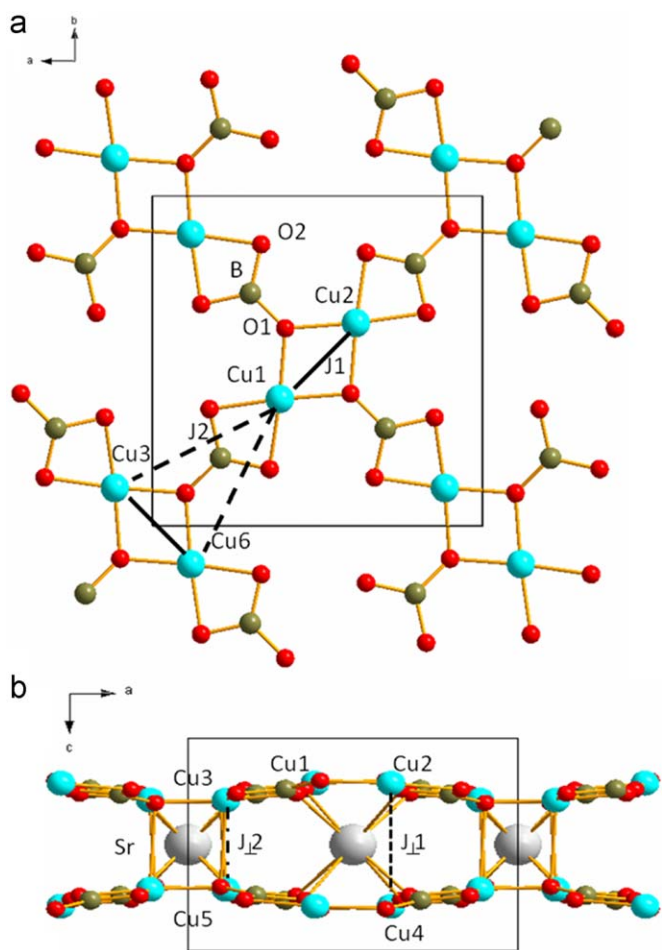


Fig. 1. Low-temperature structure of SrCu₂(BO₃)₂ projected: (a) along the *ab*-plane and (b) along the *ac*-plane. J_1 and J_2 the in-plane Cu–Cu intra-dimer and inter-dimer exchange integrals, respectively. $J_{\perp 1}$ and $J_{\perp 2}$ the out-of-plane Cu–Cu dimer interactions.

a quantum phase transition [12] is expected to take place from a dimer singlet to a plaquette singlet ground state [13]. Furthermore, the phase transition point between this intermediate, frustration-induced phase and a gapless ordered state was also estimated at $x_c \cong 0.86$ [14], while the model reduces to a square lattice Heisenberg antiferromagnet for some value of $x \gg 1$. As SrCu₂(BO₃)₂ appears to be in the vicinity of a quantum critical point that separates the dimer state from a gapless Néel ordered state, renders it a system of great interest. Among the various choices of coupling constants, the optimal set shows a critical ratio $x_c \cong 0.635$, with J_1 (Cu1–Cu2 in Fig. 1) and J_2 (Cu1–Cu3 in Fig. 1) estimated to be 85 and 54 K, respectively [15]. These parameters were shown to reproduce with accuracy both the temperature dependence of the magnetic susceptibility as well as that of the specific heat within the gap region.

Moreover, some authors have emphasized the importance of the inter-layer coupling (J_3), i.e. a Shastry–Sutherland lattice with three-dimensional (3D) interactions, in order to properly model the thermodynamic properties of this novel compound [15,16]. It has been argued that such an inter-layer coupling ($J_3/J_1 \cong 0.09$) can influence the excitation spectrum and shift the phase diagram boundary from a gapped to a Néel state [17]. Substitutions of aliovalent cations, such as Na, Al, La, Y for Sr [18] that modify the chemical pressure on the Cu–O planes or dilution of the copper sub-lattice with Zn or Mg ions [19–22] have also been reported in

the attempt to stabilise a long-range ordered antiferromagnetic (AFM) state, however, with no success so far.

The intriguing behaviour in SrCu₂(BO₃)₂ is due to its magnetic anisotropy that appears not well understood up till now. As the crystal structure is anisotropic, with a rather large J_1 exchange coupling, the main contribution to spin anisotropy was shown [23] to be of Dzyaloshinsky–Moriya (DM) type, whose presence obeys a number of rules posed by the crystal symmetry. Therefore the knowledge of the low-temperature crystal structure is crucial for the understanding of the magnetic properties of SrCu₂(BO₃)₂. While the crystal structure has been determined quite comprehensively by single crystal X-ray diffraction measurements down to 100 K [24], no structural studies have been pursued up to now at lower temperatures where novel quantum mechanical magnetic behaviour was found [6–10]. Since accurate knowledge of the lattice symmetry is necessary to rationalise the ground state properties, here we report a detailed structural study for SrCu₂(BO₃)₂ at low-temperatures. We performed high-resolution neutron powder diffraction (NPD) measurements between room temperature (RT) and down to 2 K, with emphasis in the “spin-gap” regime ($2 < T < 40$ K) [25]. Our study demonstrates the onset of subtle atomic displacements, concurrent with an unusual negative thermal expansion in the dimerized state, all postulating to delicate spin-lattice coupling effects for $T < 40$ K. This new knowledge on the SrCu₂(BO₃)₂ lattice, offers a valuable insight in view of future efforts aiming to understand how the ground state energy is minimized by lattice modifications pertaining to the rearrangement of the magnetic interactions among the Cu dimers.

2. Experimental

Single crystals of SrCu₂(¹¹BO₃)₂ have been grown from a Li¹¹BO₃-flux as described elsewhere [26]. A 4 g polycrystalline sample was produced from crashing the rods used for the single crystal growth. Neutron powder diffraction experiments were performed on the High-Resolution Powder Diffractometer (HRPD) and on the General Material Diffractometer (GEM) at the neutron spallation source ISIS (UK). The sample used for the present work was inserted in a flat rectangular sample holder (HRPD; 4 g powder) and in a 6 mm Vanadium can (GEM; 1 g powder). HRPD data were collected from room temperature to $T=2$ K, with particular interest in the low-temperature region. For $T < 100$ K, temperature steps of 4 K were used, while for $T > 100$ K, the temperature was raised in steps of 50 K. Long counting time was allowed for data collected at 2, 100 and 295 K. Measurements on GEM were performed in the temperature range $2 < T < 40$ K, on warming with temperature intervals of 1 K and high statistics. In both cases a standard ILL Orange cryostat was used. The collected patterns were analyzed with the Rietveld method. Refinements of the nuclear structure were carried out with the GSAS program suite [27].

3. Results and discussion

From the crystallographic point of view, SrCu₂(BO₃)₂ shows a second-order structural phase transition at $T_S=395$ K from space group $I4/mcm$ above T_S to a non-centrosymmetric space group $I-42m$ below T_S [24]. Below 395 K all our datasets could be refined with the proposed space group. Fig. 1 shows a representation of the structure as derived after Rietveld refinements of the room temperature HRPD data. Our structural analysis shows that layers extending in the *ab*-plane are formed by (BO₃)³⁻ groups and Cu²⁺ ($S = \frac{1}{2}$) ions, while Sr²⁺ ions separate two adjacent layers along the *c*-axis. The coordination of copper by the rigid BO₃ groups leads to

a pronounced angular distortion (corrugation) of the CuO_4 square below T_S , with important consequences on the effect of the magnetic anisotropy on the ground state properties. The nearest-neighbor (nn) copper atoms form dimers of edge-sharing CuO_4 groups, which are not co-planar at $T < T_S$ and as that the Cu-BO_3 layer is not a mirror plane for the dimers, as it used to be above T_S . Each dimer is coordinated from both sides by the two symmetry equivalent oxygens of the borate group. The dimers are orthogonally arranged with respect to each other in a topologically equivalent Shastry–Sutherland lattice arrangement.

In this lattice type each dimer becomes relatively strongly coupled to the two neighboring orthogonal dimers (next-nearest-neighbors= nnn) by super-superexchange interactions (J_2) via rigid BO_3 groups. Our structural analysis finds that these BO_3 groups do not show any appreciable temperature dependence in the T range of interest. Indeed, the B–O1 and B–O2 distances remain at values of 1.372(1) and 1.378(1) Å, respectively, while in the low- T region. The corresponding angles are also rather rigid, taking values of 122.90(5)° for O1–B–O2 and 114.2(1)° for O2–B–O2 (Fig. 1). Rigidity in planar triborate groups is frequently met in metal-borate systems. For example, in LiB_3O_5 , triborate units composed of three inequivalent B–O bonds (1.349(5), 1.367(1) and 1.396(1) Å) are connected with flexible Li–O linkages that are responsible for the anisotropic thermal expansion of the lattice [35]. In the present case, with the rigid BO_3 interconnecting the dimers, we will show that the different expansion tendency of the CuO_4 structural units allows in the $\text{SrCu}_2(\text{BO}_3)_2$ subtle modifications that could optimise interactions of different nature, such as the magnetic exchange coupling (*vide infra*).

Other crystal system changes, which were unveiled by the high resolution of the HRPD diffractometer, include a significant broadening of the Bragg reflections, inferring to distortions due to microstrain. In order to properly take this into account, a model with anisotropic strain broadening based on Stephens formalism has been incorporated in the Rietveld refinements [28]. Within this formalism, the spacing d between lattice planes for any given reflection defined by the Miller indexes hkl is $1/d^2 = Ah^2 + Bk^2 + Cl^2 + Dhk + Ehl + Fhk$, where the capital case letters represent metric parameters of the reciprocal lattice. Strain broadening here is considered as a manifestation of the distribution of these parameters. We can therefore write the contribution to the broadening on a reflection hkl due to strain as $\sigma^2(hkl)$. The variance matrix for a Gaussian distribution of these parameters can be expressed in the following way:

$$\sigma^2(hkl) = \sum_{\text{HKL}} S_{\text{HKL}} h^H k^K l^L$$

with the term S_{HKL} defined for $H+K+L=4$ ($H, K, L \geq 0$). For Laue symmetries other than -1 (triclinic), the symmetry imposes restrictions on the allowed S_{HKL} terms. Since the Laue class of the structure for this compound is $4/mmm$ (tetragonal), only 4 independent coefficients are allowed (i.e. for a tetragonal symmetry: $A=B$, $D=E=F=0$ and the corresponding anisotropic strain parameters are $S_{400}=S_{040}$, $S_{202}=S_{022}$, S_{004} , S_{220}). The refinement with this model (including strain: $\chi^2=3.415$, Bragg R -factor=4.5%, without strain: $\chi^2=12.97$ and Bragg R -factor=10% at $T=2$ K) showed large strain coefficients, such as $S_{004} \sim 1.77(4)$ and $S_{202} \sim 3.13(3)$, while others like the S_{400} and S_{220} parameters were found to be smaller ($\sim 2.28 \times 10^{-1}(5)$ and $\sim 1.24 \times 10^{-1}(7)$, respectively). Based on this analysis, we also find that the lattice strain does not seem to exhibit significant temperature dependence within the T -range investigated. The enhanced S_{HKL} parameters are an indication of defects or disorder, which in the present case appears mainly along the c -direction, as the Stephens coefficients with non-zero L index are larger. This could be an

effect of the corrugation of the ab -planes below the high- T (T_S) structural transition.

Importantly, the purpose of this study is to look for spontaneous changes in the crystal system by means of Rietveld refinements as accurate knowledge of the lattice symmetry determines the spin-anisotropies necessary to rationalise experimental observations, such as, forbidden singlet–triplet transitions in high-field ESR [29]. Along these lines it is worth noting that the data collected on the HRPD diffractometer (Fig. 2a), have revealed unusual negative thermal expansion of the lattice below $T \sim 40$ K (Fig. 2a, inset). We argue that this is primarily due to the in-plane expansion (0.02%; *vide infra*), which overcomes a slight contraction along the c -direction. The quite unusual and puzzling behaviour of $\text{SrCu}_2(\text{BO}_3)_2$ around the $T=34$ K region motivated us to study the subtle lattice changes in more detail and the results are discussed in the following paragraphs. Although the HRPD data provide reliable information on the general lattice modifications, the involved statistics do not allow for an accurate determination of the T -dependence of crystallographic

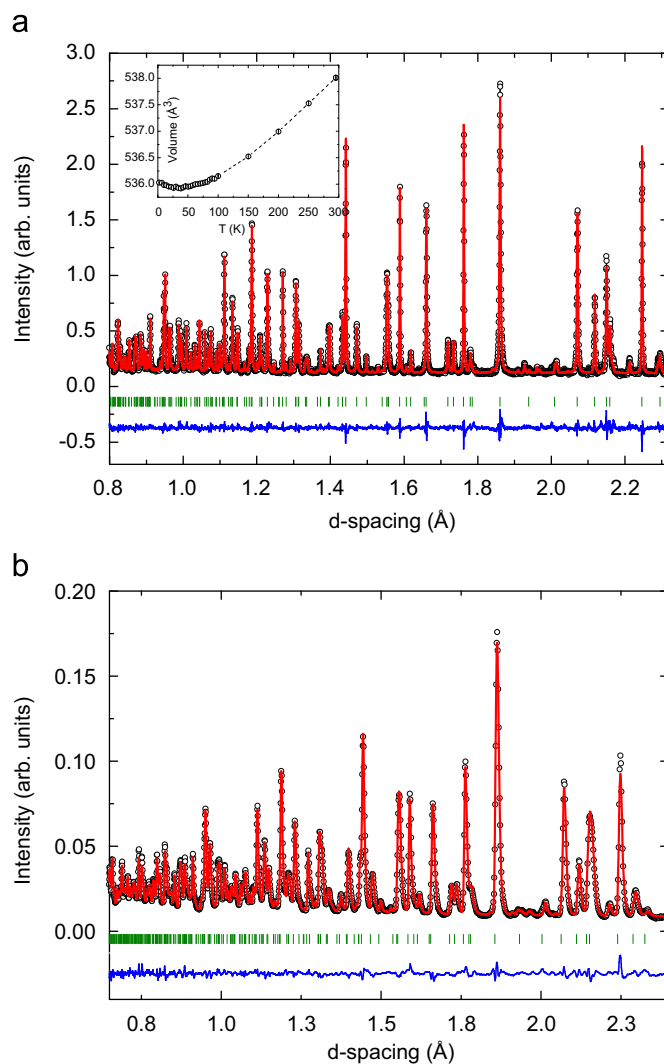


Fig. 2. Rietveld plots for (a) $T=100$ K diffraction pattern of $\text{SrCu}_2(\text{BO}_3)_2$ collected on the HRPD diffractometer. Inset: Full temperature evolution of the unit cell volume. (b) $T=2$ K diffraction pattern of $\text{SrCu}_2(\text{BO}_3)_2$ collected on the GEM diffractometer. The black dots represent the data, red line is the calculated pattern fitted to the data, while the blue line at the bottom of the plot is the difference between calculated and observed. The green vertical marks indicate the position of the Bragg reflections. For interpretation of the references to colour in this figure legend, the reader is referred to the web version of this article.

parameters, such as bond lengths, bond angles and thermal parameters, which can all reflect local lattice adjustments.

In order to derive precise crystallographic information and observe structural deformations pertaining to the spin-gap region, datasets were recorded on the GEM diffractometer (Fig. 2b) below $T=40$ K. We observe an expansion in the ab -plane and contraction in the c -axis (corresponds to volume expansion of 0.02%; Fig. 3), in agreement with the earlier HRPD work. Table 1 summarizes the lattice parameters and atomic positions from the $T=2$ and 40 K GEM datasets, respectively. Fig. 4a shows the temperature dependence of the intra-dimer (Cu1–O1–Cu2) angle (Fig. 1). This angle significantly increases from about $98.02(7)^\circ$ at 40 K to about $98.49(7)^\circ$ at 2 K. At the same time, the intra-dimer Cu1–Cu2 distance (Fig. 1) expands, changing from $2.916(2)\text{Å}$ at 40 K to $2.930(2)\text{Å}$ at 2 K (Fig. 4b).

The increase of the Cu1–Cu2 distance is directly related to the lattice expansion in the ab -plane (Fig. 3a). This is partially balanced by a shortening of the Cu1–Cu3 inter-dimers distances (Fig. 4c). Very interestingly, we observed that the bending angle between the CuO_4 groups (Fig. 4d), defined by the angle formed by two adjacent CuO_4 groups along the $[110]$ direction, decreases when the temperature is lowered and the planes become less corrugated at base temperature (~ 2 K). This “flattening” of the 2D planes leads to an increase of the short inter-dimer distances (Cu3–Cu5; Fig. 5a) between adjacent layers, while the long inter-

Table 1

Atomic positions obtained from full profile Rietveld refinements of the GEM powder diffraction data of $\text{SrCu}_2(\text{BO}_3)_2$.

Atom	Wyckoff pos	x/a	y/b	Z/c	Occ.	B_{iso}
(a)						
Sr	4c	0	1/2	0	1.0	0.07(2)
Cu	8i	0.11535(7)	0.11535(7)	0.2895(2)	1.0	0.05(2)
B	8i	0.29499(8)	0.29499(8)	0.2386(2)	1.0	0.02(2)
O1	8i	0.40081(9)	0.40081(9)	0.1973(2)	1.0	0.12(2)
O2	16j	0.32811(7)	0.14604(8)	0.2591(2)	1.0	0.10(2)
(b)						
Sr	4c	0	1/2	0	1.0	0.10(3)
Cu	8i	0.11482(7)	0.11482(7)	0.2894(2)	1.0	0.09(3)
B	8i	0.29463(8)	0.29463(8)	0.2380(2)	1.0	0.02(2)
O1	8i	0.40049(9)	0.40049(9)	0.1964(2)	1.0	0.13(3)
O2	16j	0.32780(8)	0.14578(8)	0.2586(2)	1.0	0.14(2)

(a) $T=2$ K. Lattice parameters: $a=8.98493(6)\text{Å}$, $c=6.64117(8)\text{Å}$, $V=536.135(8)\text{Å}^3$. Weighted profile $R_{\text{wp}}(\%)=3.95$, Profile $R_p(\%)=3.70$, Bragg R -factor $(\%)=4.47$, $\chi^2=13.99$. (b) $T=40$ K. Lattice parameters: $a=8.98354(6)\text{Å}$, $c=6.64229(8)\text{Å}$, $V=536.059(8)\text{Å}^3$. Weighted profile $R_{\text{wp}}(\%)=3.92$, Profile $R_p(\%)=3.76$, Bragg R -factor $(\%)=4.3$, $\chi^2=14.71$. Estimated standard errors at the last significant digit are given in parenthesis.

dimer distances (Cu2–Cu4; Fig. 5b) do not change significantly in the spin-gap region. Planar CuO_4 groups are common in 2D cuprates such as the Bi_2CuO_4 system [36]. In this long-range antiferromagnetically ordered system, where superexchange interactions play a major role, Cu–Cu distances are about $2.899(3)\text{Å}$ (namely slightly shorter than in $\text{SrCu}_2(\text{BO}_3)_2$), while the O–Cu–O angles are much closer to 90° (i.e. $89.89(3)^\circ$) with respect to those (i.e. $\sim 81.28(7)^\circ$) measured in $\text{SrCu}_2(\text{BO}_3)_2$. The geometry of the staggered CuO_4 groups in Bi_2CuO_4 does not support cation–anion–cation exchange interactions, but super-superexchange interactions involving two oxygen atoms. Such interactions have been invoked as being responsible for short-range order along the chains. These short-range correlations determine the observed antiferromagnetic behaviour that relates Cu atoms belonging to different chains.

Let us now consider the effect of inter- and intra-dimer exchange interactions on the lattice and the distortions therefore observed in $\text{SrCu}_2(\text{BO}_3)_2$. Below 34 K, the leading interaction that modifies the nuclear structure of $\text{SrCu}_2(\text{BO}_3)_2$ is the isotropic magnetic exchange. Indeed, the opening of the Cu1–O1–Cu2 angle (Fig. 4a) and the increase of the Cu1–Cu2 dimer distances (Fig. 4b), while BO_3 side groups remain unmodified at low- T (*vide infra*), suggest a strengthening of the intra-dimer superexchange (J_1). If we assume AFM spin arrangement of the Cu moments within each dimer, the application of Goodenough–Kanamori–Anderson (G–K–A) rules [30] would suggest enhanced mn (J_1) exchange integrals (Fig. 1). Interestingly, in $\text{SrCu}_2(\text{BO}_3)_2$, the inter-dimer exchange path (which contains the rigid BO_3 groups) shrinks (Fig. 4c), showing an opposite trend compared to the intra-dimer one that elongates (Fig. 4b). All the lattice changes occur while crossing-over into the spin-gap regime. We therefore assume that at low enough temperature significant spin-lattice coupling is established when the concentration of triplets increases (with increasing T). This will tend to minimize the intra-dimer exchange; hence the shrinkage of the lattice (due to a reduction of the Cu–O–Cu angle) with increasing temperature, before the natural thermal expansion takes over. Consequently, the enhanced spin–lattice coupling leads to the observed negative thermal expansion of 0.02% in the ab -plane (Fig. 3).

In support to this behaviour comes a recent synchrotron X-ray diffraction study where lattice contraction in $\text{SrCu}_2(\text{BO}_3)_2$ has been also observed when the strength of an intense applied magnetic field is raised at low-temperatures (1.5 K). This tuneable

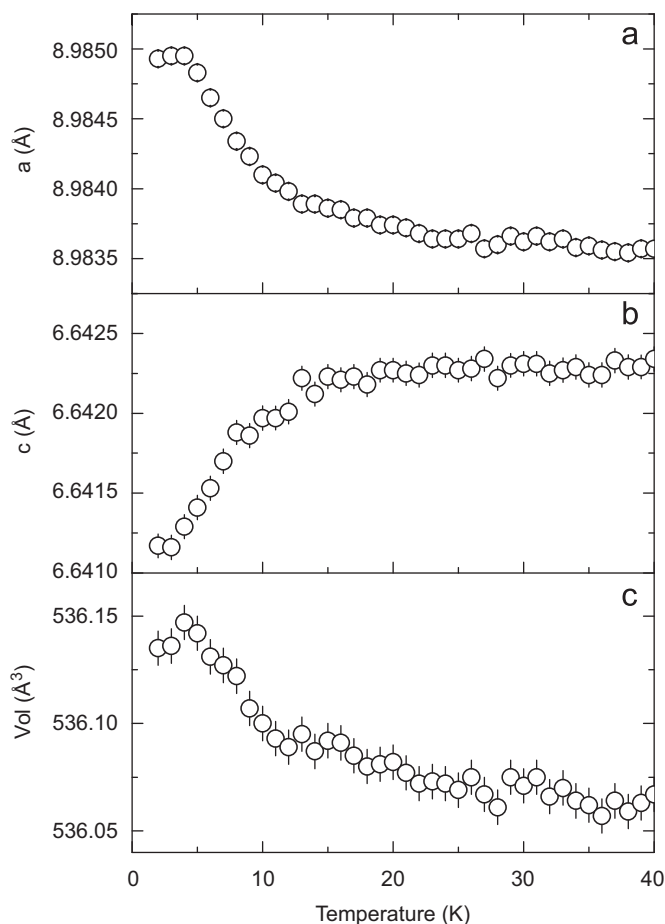


Fig. 3. Temperature evolution of the Rietveld refined lattice parameters in the low-temperature range ($2 \leq T \leq 40$ K; GEM diffractometer) of the $\text{SrCu}_2(\text{BO}_3)_2$. (a) The tetragonal a and b crystallographic directions; an unusual in-plane expansion is resolved. (b) The c crystallographic direction; an out-of-plane contraction takes place. (c) The unit cell volume; negative thermal expansion is uncovered within the spin-gap region.

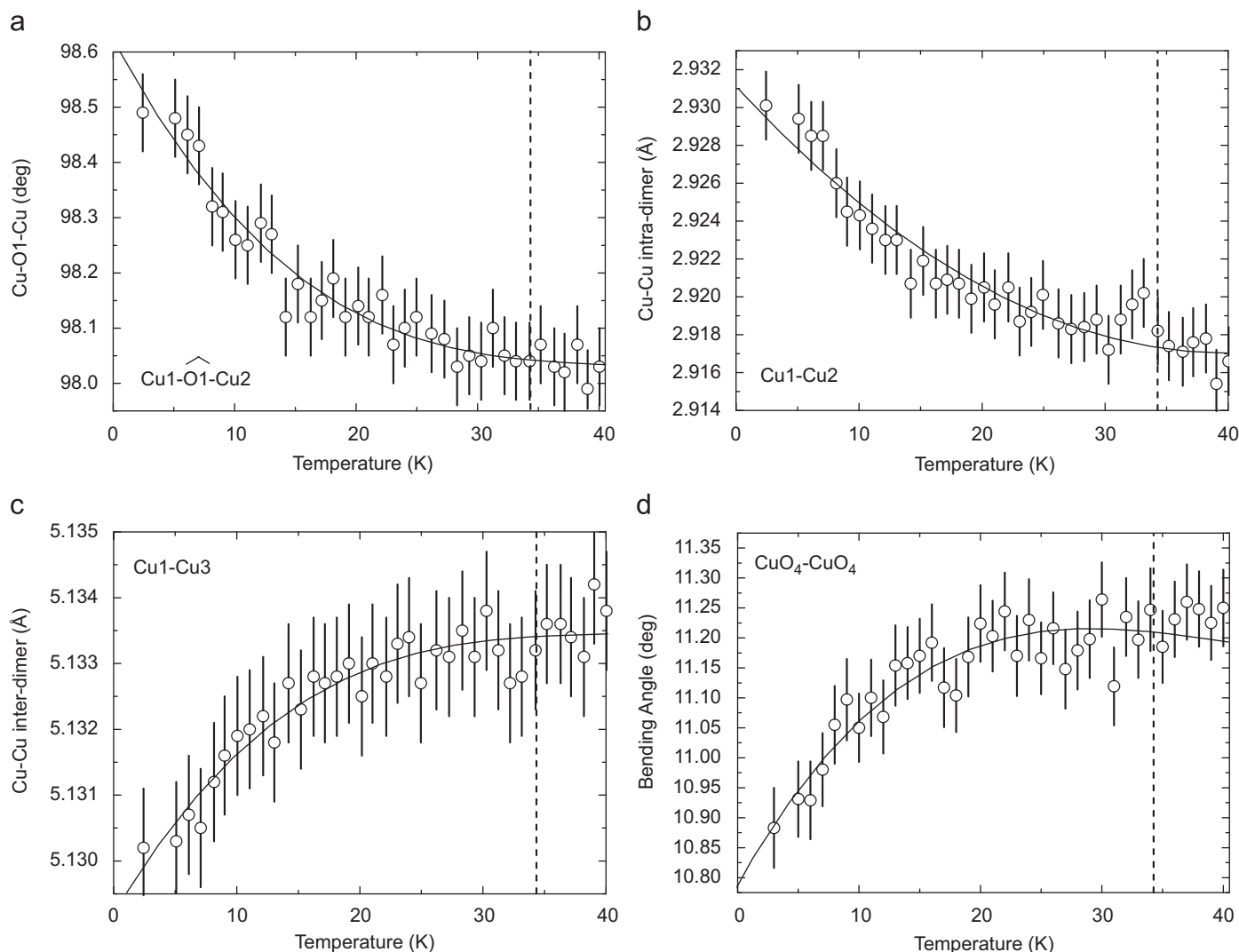


Fig. 4. Temperature dependence of: (a) intra-dimer exchange pathway angle $\text{Cu1}-\hat{\text{O}}_1-\text{Cu2}$. (b) The intra-dimer $\text{Cu1}-\text{Cu2}$ distances. (c) The inter-dimer $\text{Cu1}-\text{Cu3}$ distances, (d) the layer corrugation, defined as the angle between neighboring CuO_4 groups within each layer in $\text{SrCu}_2(\text{BO}_3)_2$. The vertical dashed line in each one of the plots marks the entering into the spin-gap region.

parameter also increases the population of triplets as does the temperature increase [34] and the authors reported the observation of a close relationship between the lattice constants and magnetization. They found a variation of the in-plane lattice constant with an applied field, B_i , of the order of $-\Delta a/a = [a(B_0) - a(B_i)]/a(B_0) \sim 0.5 \times 10^{-4}$ at 30 T, 1×10^{-4} at 35 T. Very interestingly, their findings are in agreement with our structural measurements for the temperature dependence of the basal plane lattice parameters, which result in changes ($-\Delta a/a = [a(T=2\text{K}) - a(T)]/a(T=2\text{K})$) of the same order of magnitude, namely, 0.5×10^{-4} at 7 K, 1×10^{-4} at 10 K and 1.2×10^{-4} at 35 K.

Together with the effect of the frustrated, isotropic super-exchange interactions (J_1, J_2) on the lattice, it is worth considering the influence of two possible weaker interactions to the spin gap, namely the inter-layer coupling J_3 and the magnetic anisotropy. The latter involves the antisymmetric Dzyaloshinsky–Moriya interaction $\mathbf{D} \cdot (\mathbf{S}_i \times \mathbf{S}_j)$, where $\mathbf{S}_i, \mathbf{S}_j$ represent the spins at neighboring sites [23], that justifies the fine structure of the excited triplet state and its unusual magnetic field dependence [31,32]. In the $\text{SrCu}_2(\text{BO}_3)_2$ structure, a center of inversion at the middle of the dimer bond forbids the intra-dimer DM interaction ($T > T_S$), and instead the inter-dimer out-of-plane DM interaction evolves as the dominant one. When we lower the temperature, the

inversion center of symmetry is lost at the $I4/mcm$ to $I-42m$ structural transition [11,24] and another DM component may play a role. Namely the nn intra-dimer DM interaction can become important, which has been suggested as a pathway to account for forbidden singlet–triplet transitions in high-field ESR [29,33]. From the analysis of the present NPD data ($T < T_S$), we find that the lattice symmetry does not preclude nn ($\text{Cu1}-\text{Cu2}$) DM interactions. When we enter the spin-gap region ($< 34\text{K}$), the in-plane structure becomes more rigid due to the strengthening of intra-dimer interactions (*vide supra*). Such a modification of the crystal lattice leads to a decrease of the observed planar buckling, but the mirror plane lost below T_S is not recovered, meaning that nn DM interactions are still a feasible mechanism.

Furthermore, we realize that weak three-dimensional exchange interactions can also develop in the system through the flattening of the ab -plane ($< 34\text{K}$), as evidenced by the increase of the $\text{Cu3}-\text{Cu5}$ ion distances (Fig. 5a) that correspond to the short inter-dimer separation between the layers. On the contrary, the long inter-dimer distances ($\text{Cu2}-\text{Cu4}$; Fig. 5b) remain almost unaltered below $T=34\text{K}$. The two types of inter-layer couplings ($J_{\perp 1}, J_{\perp 2}$; Fig. 1b) that are established herein, have been estimated to range from $J_{\perp}/J_1 \sim 0.094$ to 0.21 [15,16]. As they are relatively weaker with respect to the corresponding in-plane exchange

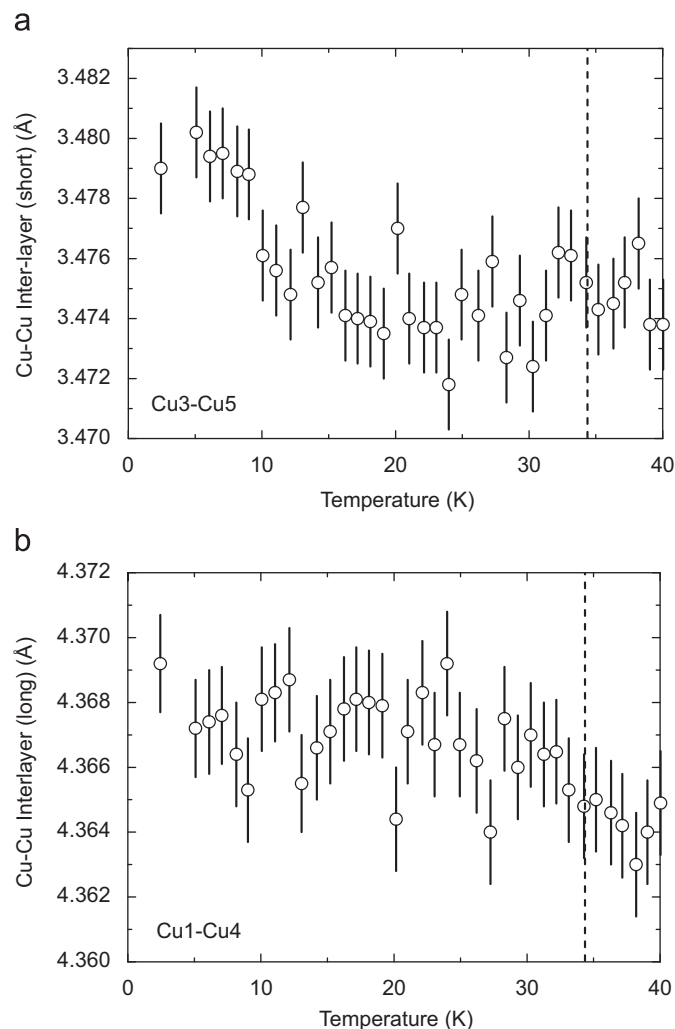


Fig. 5. Temperature evolution of: (a) the short inter-layer distances, between Cu3–Cu5 sites and (b) the long inter-layer distances, between Cu1–Cu4 sites in adjacent Cu– BO_3 planes of the $\text{SrCu}_2(\text{BO}_3)_2$. The vertical dashed line in each one of the plots marks the entering into the spin-gap region.

integrals, they are expected to play a minor role in the observed structural distortions.

The current NPD data analysis finds small crystal system changes that do not violate restrictions posed by the tetragonal $I-42m$ lattice symmetry of $\text{SrCu}_2(\text{BO}_3)_2$. A comprehensive theoretical study, based on the structural modifications described in this work is desirable. We expect that it will improve the understanding of the temperature evolution of the exchange coupling integrals and the role of magnetic anisotropy within the spin-gap region.

4. Conclusions

We performed extensive high-resolution, high-statistics neutron powder diffraction measurements on the two-dimensional quantum antiferromagnet $\text{SrCu}_2(\text{BO}_3)_2$, between room temperature and down to 2 K. Subtle spin–lattice coupling was unveiled in the low-temperature region (< 34 K), where the spin-singlet state populates and characterises the ground state properties. The Rietveld analysis of the NPD data revealed an unusual negative thermal expansion of the lattice, which reflects upon subtle lattice adjustments without space group symmetry ($I-42m$) change. The dimerization of the Cu–Cu ions, mapping onto an orthogonal spin-

dimer system and the concurrent widening of the angle connecting nearest-neighbour Cu sites, suggests the strengthening of the intra-dimer antiferromagnetic interactions. We find that the increase in the intra-dimer separation changes quite significantly the structure. The novel orthogonal arrangement of the dimers leads to a net expansion in the ab -plane and a reduction to the in-plane inter-dimer distances. These lattice distortions that take place at low enough temperatures (< 34 K) are not exclusive to in-plane modifications. Importantly, the buckling of the copper–borate planes is also modified. The structural analysis suggests that the out-of-plane coupling strengthen somehow, due to the shrinkage along the c -direction. It reflects a more three-dimensional type of behaviour for the $\text{SrCu}_2(\text{BO}_3)_2$ lattice within the spin-gap temperature region. At low-temperatures (< 34 K), the rules posed by the crystal symmetry ($I-42m$) on the Cu dimers allow for Dzyaloshinsky–Moriya (DM) coupling of the magnetic moments. Our analysis suggests that DM interactions remain a crucial spin anisotropy for understanding the intriguing $\text{SrCu}_2(\text{BO}_3)_2$ magnetic behaviour.

Acknowledgements

We would like to thank R.M. Ibberson for help with the experiments. AL acknowledges partial support from the European Commission (“Construction of New Infrastructures”, ISIS Target Station II, contract no. 011723), and the EU access to research infrastructures program of ISIS (Project Reference: HPRI-CT-2001-00116). This work was partially supported by Grants-in-Aid for Science Research on Priority Areas “Novel States of Matter Induced by Frustration” (No. 19052004) from the Ministry of Education, Culture, Sports, Science and Technology of Japan.

Appendix. Supporting Information

Supplementary data associated with this article can be found in the online version at doi:10.1016/j.jssc.2009.09.017.

References

- [1] J. Darriet, J.P. Regnault, *Solid State Commun.* 86 (1993) 409.
- [2] M. Hase, I. Terasaki, K. Uchinokura, *Phys. Rev. Lett.* 70 (1993) 3651.
- [3] M. Azuma, Z. Hiroi, M. Takano, K. Ishida, Y. Kitaoka, *Phys. Rev. Lett.* 73 (1994) 3463.
- [4] S. Taniguchi, T. Nishikawa, Y. Yasui, Y. Kobayashi, M. Sato, T. Nishioka, M. Kontani, K. Sano, *J. Phys. Soc. Jpn.* 64 (1995) 2758.
- [5] B.S. Shastry, B. Sutherland, *Physica B* 108 (1981) 1069.
- [6] H. Kageyama, K. Yoshimura, R. Stern, N.V. Mushnikov, K. Onizuka, M. Kato, K. Kosuge, C.P. Slichter, T. Goto, Y. Ueda, *Phys. Rev. Lett.* 82 (1999) 3168.
- [7] K. Kodama, M. Takigawa, M. Horvatic, C. Berthier, H. Kageyama, Y. Ueda, S. Miyahara, F. Becca, F. Mila, *Science* 298 (2002) 395.
- [8] H. Nojiri, H. Kageyama, K. Onizuka, Y. Ueda, M. Motokawa, *J. Phys. Soc. Jpn.* 68 (1999) 2906.
- [9] H. Kageyama, M. Nishi, N. Aso, K. Onizuka, T. Yosihama, K. Nukui, K. Kodama, K. Kakurai, Y. Ueda, *Phys. Rev. Lett.* 84 (2000) 5876.
- [10] H. Kageyama, K. Onizuka, T. Yamauchi, Y. Ueda, S. Hane, H. Mitamura, T. Goto, K. Yoshimura, K. Kosuge, *J. Phys. Soc. Jpn.* 68 (1999) 1821.
- [11] S. Miyahara, K. Ueda, *J. Phys.: Condens. Matter* 15 (2003) R327.
- [12] S. Miyahara, K. Ueda, *Phys. Rev. Lett.* 82 (1999) 3701.
- [13] Z. Weihong, J. Oitmaa, C.J. Hamer, *Phys. Rev. B* 60 (1999) 6608; E. Müller-Hartmann, R.R.P. Singh, C. Knetter, G.S. Uhrig, *Phys. Rev. Lett.* 84 (2000) 1808.
- [14] A. Koga, N. Kawakami, *Phys. Rev. Lett.* 84 (2000) 4461.
- [15] S. Miyahara, K. Ueda, *J. Phys. Soc. Jpn. (Suppl.) B* 69 (2000) 72.
- [16] C. Knetter, A. Buhler, E. Müller-Hartmann, G.S. Uhrig, *Phys. Rev. Lett.* 85 (2000) 3958.
- [17] A. Koga, *J. Phys. Soc. Jpn.* 69 (2000) 3509.
- [18] G.T. Liu, J.L. Luo, N.L. Wang, X.N. Jing, D. Jin, T. Xiang, Z.H. Wu, *Phys. Rev. B* 71 (2005) 014441.
- [19] G.T. Liu, J.L. Luo, Y.Q. Guo, S.K. Su, P. Zheng, N.L. Wang, D. Jin, T. Xiang, *Phys. Rev. B* 73 (2006) 014414.

- [20] A. Fukaya, Y. Fudamoto, I.M. Gat, T. Ito, M.I. Larkin, A.T. Savici, Y.J. Uemura, P.P. Kyriakou, G.M. Luke, M.T. Rovers, H. Kageyama, Y. Ueda, *Physica B* 326 (2003) 446.
- [21] S. Haravifard, S.R. Dunsiger, S.E. Shawish, B.D. Gaulin, H.A. Dabkowska, M.T.F. Telling, T.G. Perring, J. Bonca, *Phys. Rev. Lett.* 97 (2006) 247206.
- [22] A. Lappas, A. Schenck, K. Prassides, *Physica B* 326 (2003) 431.
- [23] O. Cépas, K. Kakurai, L.P. Regnault, T. Ziman, J.P. Boucher, N. Aso, M. Nishi, H. Kageyama, Y. Ueda, *Phys. Rev. Lett.* 87 (2001) 167205.
- [24] K. Sparta, G.J. Redhammer, P. Roussel, G. Heger, G. Roth, P. Lemmens, A. Ionescu, M. Grove, G. Guntherodt, F. Hüning, H. Lueken, H. Kageyama, K. Onizuka, Y. Ueda, *Eur. Phys. J. B* 19 (2001) 507.
- [25] For clarity in the discussion we define the region below $T=34$ K as the “spin gap” regime to address the structural and magnetic changes that occur as a consequence of the modification in population of the singlet and triplet states. We therefore use this terminology throughout the manuscript.
- [26] H. Kageyama, K. Onizuka, T. Yamauchi, Y. Ueda, *J. Crystal Growth* 206 (1999) 65.
- [27] A.C. Larson, R.B.V. Dreele, General Structure Analysis System (GSAS), Los Alamos National Laboratory Report LAUR 86-748, 1994.
- [28] P.W. Stephens, *J. Appl. Crystallogr.* 32 (1999) 281.
- [29] H. Nojiri, H. Kageyama, Y. Ueda, M. Motokawa, *J. Phys. Soc. Jpn.* 72 (2003) 3243.
- [30] J. Goodenough, A. Wold, R.J. Arnett, N. Menyuk, *Phys. Rev.* 124 (1961) 373.
- [31] A. Zorko, D. Arcon, H. van Tol, L.C. Brunel, H. Kageyama, *Phys. Rev. B* 69 (2004) 174420.
- [32] A. Zorko, D. Arcon, H. Kageyama, A. Lappas, *Appl. Magn. Reson.* 27 (2004) 267.
- [33] G.A. Jorge, R. Stern, M. Jaime, N.H. nd J. Bonca, S.E. Shawish, C.D. Batista, H.A. Dabkowska, B.D. Gaulin, *Phys. Rev. B* 71 (2005) 092403.
- [34] Y. Narumi, N. Terada, Y. Tanaka, M. Iwaki, K. Katsumata, K. Kindo, H. Kageyama, Y. Ueda, H. Toyokawa, T. Ishikawa, H. Kitamura, *J. Phys. Soc. Jpn.* 78 (2009) 043702.
- [35] Yu.F. Shepelev, R.S. Bubnova, S.K. Filatov, N.A. Sennova, N.A. Pilneva, *J. Solid State Chem.* 178 (2005) 2987.
- [36] J.L. Garcia-Munoz, J. Rodriguez-Carvajal, F. Sapina, M.J. Sanchis, R. Ibanex, D. Beltran-Porter, *J. Phys.: Condens. Matter* 2 (1990) 2205.